EFFECT OF TEMPERATURE ON THE IRON SULPHUR RATIO OF PYRITE DEPOSITED BY AEROSOL ASSISTED CHEMICAL VAPOUR DEPOSITION METHOD

S.O. Ezeonu (Corresponding author)
Department of Physics and Industrial Physics, Nnamdi Azikiwe University
P.M.B 5025, Awka, Anambra State, Nigeria.
E-mail: so.ezeonu@unizik.edu.ng

C.I. Nweze
Department of Physics and Industrial Physics, Nnamdi Azikiwe University
P.M.B 5025, Awka, Anambra State, Nigeria.
E-mail: ci.nweze@unizik.edu.ng

The research is sponsored by Tertiary Education Trust Fund (TETFund) of Nigeria

Abstract:Pyrite semiconducting film was deposited on a glass substrate from a single source precursor (Fe $(S_2CN(Et)_2)_3$) using aerosol assisted chemical vapour deposition AACVD. The p-XRD pattern of the deposited films shows that pure pyrite was deposited at 300^oC whereas mixture of pyrite and marcasite was deposited at 350^oC, 400^oC and 450^oC. EDX analysis shows that semiconducting pyrite was deposited at 300^oC and 350^oC, whereas metallic pyrite was deposited at 400^oC and 450^oC.

Keyword:EDX, XRD, SEM, semiconducting pyrite, metallic pyrite, AACVD.

1. INTRODUCTION

Iron pyrite (cubic FeS2) is a promising photovoltaic (PV) material and has some properties that makes it suitable for photovoltaic application, these solid state properties include, indirect band gap of 0.98eV, optical absorption coefficient of $10^5 cm^{-1}$(for λ <900 nm), adequate minority carrier diffusion length of (100-1000) nm, essentially infinite elemental abundance, high photocurrent and high quantum efficiencies[1-6]. Pyrite solar cell has some advantages over other photovoltaic materials such as cheap, nontoxic and could make a significant impact even with lower efficiencies, because most of the materials reported as photovoltaic use either toxic or not very abundant elements such as cadmium, lead or indium, etc[7]which means that these materials cannot contribute significantly to a future energy supply.Recent estimates of the annual electricity potential as well as material extraction costs and environmental friendliness led to the identification of materials that could be used in photovoltaic applications on a large scale[8] The most promising materials include iron and copper sulfides. Various methods have been used to deposit pyrite, such as, flash evaporation[9], metal organic chemical vapour deposition[1], vacuum thermal evaporation[10], ion beam and reactive sputtering[11], chemical vapour deposition[12], electrodeposition[13] and molecular beam deposition[14]. Other methods includechemical spray pyrolysis[15], vapour transport[16], hot injection method[17], sulphurization of iron oxides[18], and plasma assisted sulphurization of iron[19]. Each technique of thin film deposition has its own advantages and disadvantages. Herein, we used solution based method, precisely Aerosol Assisted Chemical Vapour Deposition (AACVD) method to deposit nanocrystalsof pyrite from a solution using single source precursor that is Diethyldithiocarbamato iron (III) $(FeS_2CN(Et)_2)_3$) and characterized the deposited films using XRD and EDX to determine the structure and iron-sulphur ratio of the deposited films. We have previously reported optical properties of pyrite

deposited by AACVD from Diethyldithiocarbamato iron (III) and in this research work,we reported the effect of depositing temperature on iron-sulphur ratio.

2. EXPERIMENTAL

All reagents were used as purchased and solvents were distilled prior to use. All syntheses were performed under an inert atmosphere of dry nitrogen using standard schlenk techniques. Elemental analysis was performed by the University of Manchester micro-analytical laboratory. Mass spectra were recorded on a Kratos concept 1S instrument. Infra-red spectra were recorded on a Specac single reflectance ATR instrument (4000-400 cm^{-1}, resolution 4 cm^{-1}). Melting points were recorded on a Barloworld SMP10 Melting Point Apparatus. p-XRD studies were performed on an Xpertdiffractometer using Cu-Kα radiation. The samples were mounted flat and scanned between 20^{o}and 70^{o} with a step size of 0.05^{o} and various count rates. Films were carbon coated using an Edward's E306A coating system before carrying out EDX analysis. EDX was carried out using a DX4 instrumentmounted on Philips XL30 field emission gun scanning electron microscope (FEGSEM)).

2.1 Precursor synthesis

The precursor, Diethyldithiocarbamato iron (III) was prepared as described previously by Paul O'Brien group and Nair*et al* 2001[20,21,22]

2.2. Preparation of solution

The solution was prepared by dissolving 0.3g (0.6 mmol) of the precursor ($FeS_2CN(Et)_2)_3$)in 15ml of toluene in a two-necked 100ml round bottom flask and concentration of 0.04mol/$dm^3$was achieved. The substrates used were glass microscope slides. The glass slides were cut to size approximately 1 x 2 cm^2 by hand. The substrates were not handled with bare fingers rather with hand gloves to avoid contamination. The substrates were cleaned with detergent solutions, rinsed with distilled water and then rinsed with acetone, methanol and distilled water and finally dried before use.

2.3. Deposition of thin films of Pyrite by AACVD

15ml of the solution was poured into the two-necked round bottom flask with a gas inlet that allowed argon (carrier gas) to pass into the solution to aid the transport of the aerosol. A piece of reinforced tubing was used to connect the flask to the reactor tube. Platon flow gauge was used to control argon flow rate. Seven glass substrates (approximately 1 x 2 cm^2) were placed inside the reactor tube which is placed in a Carbolite furnace maintained at a certain temperature. The precursor solution in a two-necked round bottom flask was kept in a water bath above the piezoelectric modulator of a PIFCO ultrasonic humidifier (Model No 1077). The solution was evaporated and the generated aerosol droplets of the precursor were transferred into the hot wall zone of the reactor by the carrier gas. This precursor vapour reached the heated substrate surface where thermally induced reactions and film deposition took place at 60mins and a particular temperature. The temperature of the Carbolite furnace was varied in step of 50^{o}C starting from 300^{o}C to 450^{o}C. The time was kept at 60mins, the flow rate kept at 160sccm and the concentration kept at 0.04mol/dm3 throughout the experiment. The experiment was repeated a good number of times, **Table 1** summarized the parameter that was varied during the deposition.

S/N	Slide No	Argon flow rate (sccm)	Concentration of precursor (mol/dm^3)	Time of deposition (minutes)	Temperature of deposition (^{o}C)	Repeated times
1	E	160.00	0.04	60.00	300.00	3
2	F	160.00	0.04	60.00	350.00	3
3	G	160.00	0.04	60.00	400.00	3
4	H	160.00	0.04	60.00	450.00	3

Table 1 Variation of temperature at 60 minutes and 0.04mol/dm^3

3. RESULTS AND DISCUSSION

3.1 XRD PATTERN OF THE FILMS

The **p-XRD** patterns of the deposited films are shown in **Figure 1.** From**Figure 1,** the vertical line represents the standard cubic pyrite ($FeS_{1.96}$ (ICDD No. 01-073-8127)). The film deposited at 300^{o}C (slide E) corresponds to pure polycrystalline pyrite with no trace of marcasite peak, whereas the films deposited at 350^{o}C (slide F), 400^{o}C (slide G) and 450^{o}C (slide H) show mixture of polycrystalline pyrite and marcasite. The marcasitic peak increases as the deposition temperature increases. The peaks at 26.3^o, 39.2^o, 52.1^o (2θ) correspond to marcasitic peak (ICDD No. 04-003-2016). Major diffraction peaks of the films deposited, both pure and impure pyrite, lies on (111), (200), (210), (211), (220), (311) and (032) planes of reflection, with the preferred orientation 0n (200) plane of reflection.

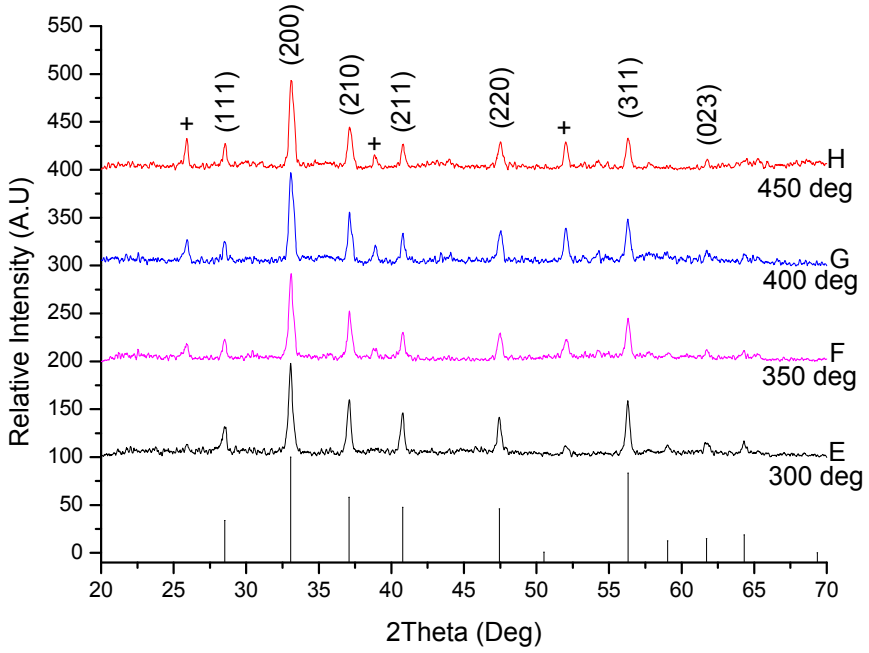

Figure 1.p-XRD patterns of deposited films, at 300^{o}C (slide E) pure polycrystalline pyrite ($FeS_{1.96}$ (ICDD No. 01- 073-8127) is formed with planes of reflection on (111), (200), (210), (211), (220),

(311) and (023), at 350°C (slide F), 400°C (slide G), 450°C (slide H) mixture of pyrite and marcasite (+) (ICDD No. 04-003-2016) is formed.

3.2 EDX OF THE FILMS

The EDX analysis of all the films shows the presence of Iron and Sulphur **Figure 2**. Quantification of iron and sulphur in the films shows that ratio of iron and sulphur increases with temperature. The Iron:Sulphur ratiois approximately 50:50 at 300°C and 350°C, 60:40 at 400°C and 64:36 at 450°C **(Table 2)**this result compares well with the work of Masood*et al* 2012[23] who reported iron sulphur ratio of 50:50 at 350°C, 50:49 at 400°C and 78:21 at 450°C for (Fe ($S_2CNEt^iPr)_3$) single source precursor deposited on silicon substrate. This result shows that the deposited semiconducting film changes from semiconducting to metallic film at high temperature. The observed sulphur deficiency at elevated temperature is attributed to the fact that sulphur evaporates from thin films at high temperatures[23,24]and its likely to depend on the nature of the substrate used.

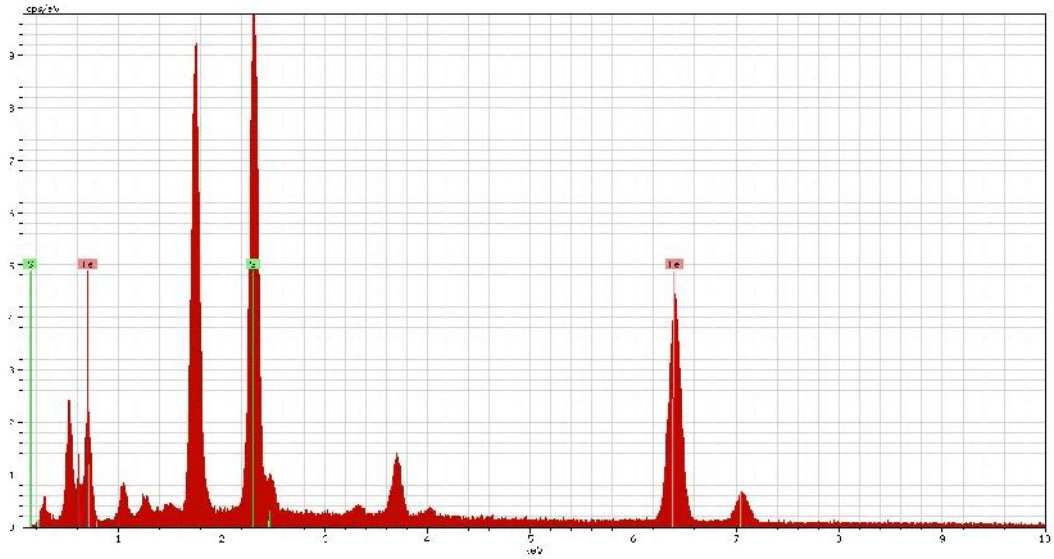

Figure 2 EDX spectrums of all the films deposited from complex (Fe ($S_2CN(Et)_2)_3$). The films show the presence of Iron (pink colour) and Sulphur (light green colour).

Deposition time (minutes)	Temperature							
	300°C		350°C		400°C		450°C	
	Fe %	S %	Fe %	S %	Fe %	S %	Fe %	S %
60	48	52	50	50	60	40	70	30

Table 2 The iron:sulphur ratio for the films deposited at 300°C, 350°C, 400°C and 450°C.

3.3 SEM IMAGES OF THE FILMS

The SEM images from the films deposited are shown in **Figures 3, 4, 5 and 6** for the film deposited at 300^{o}C, 350^{o}C, 400^{o}C and 450^{o}C respectively. At 300^{o}C, the SEM image shows irregular shape crystallites (**Figure 3**), at 350^{o}C, clusters of hexagonal plates and irregular shape crystallites is formed (**Figure 4**). At 400^{o}C flower like clusters were deposited and it is observed that some crystallites are in the process of transformation (**Figure 5**) whereas at 450^{o}Csheet like crystallites were deposited (**Figure 6**).

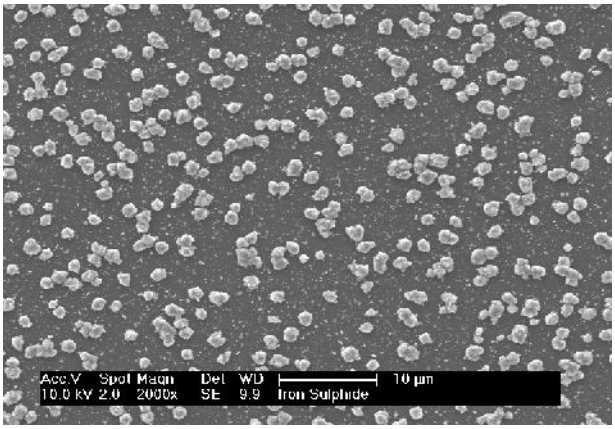

Figure3SEM image of iron sulphide (pyrite $FeS_{1.96}$) deposited at 300^{o}C

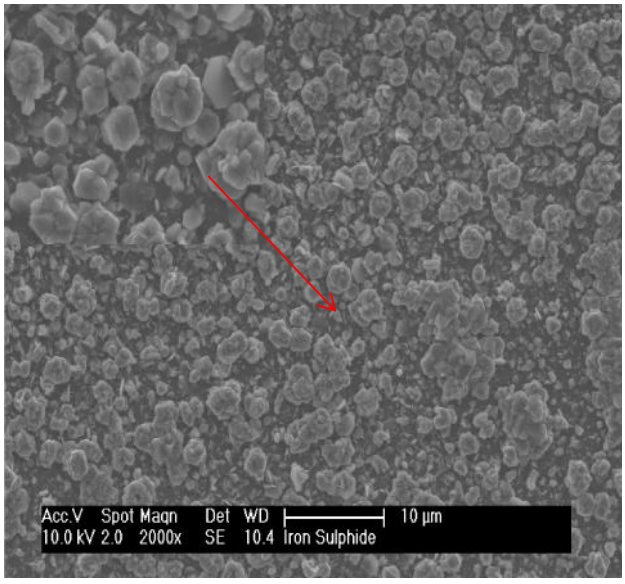

Figure 4 SEM image of iron sulphide (pyrite $FeS_{1.96}$) deposited at 350^{o}C

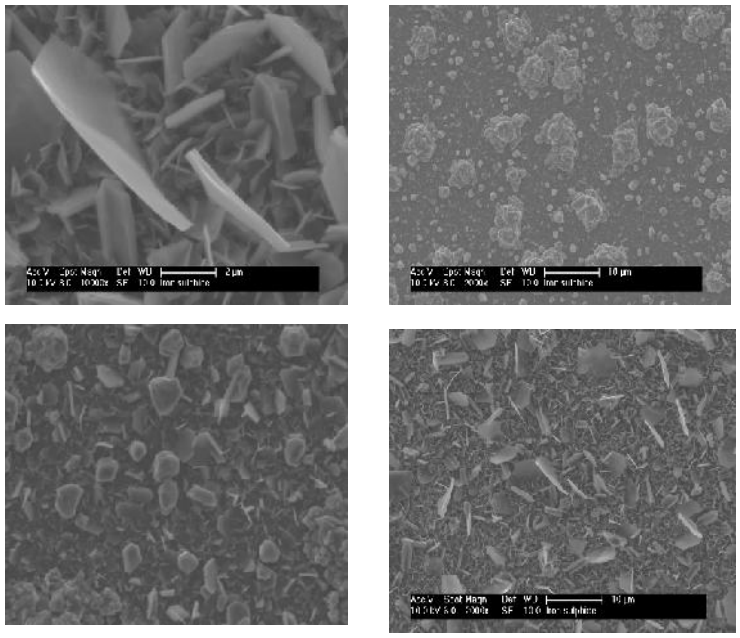

Figure 5 SEM image of iron sulphide (pyrite $FeS_{1.96}$) deposited at 400^{o}C

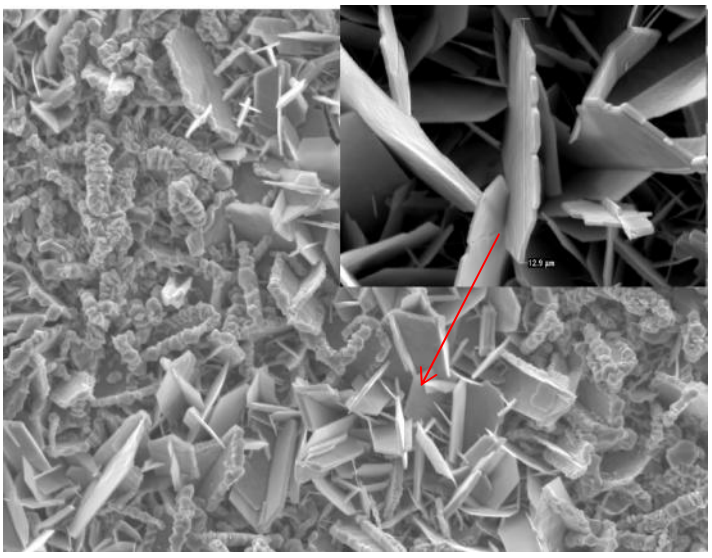

Figure 6 SEM image of iron sulphide (pyrite $FeS_{1.96}$) deposited at 450^{o}C

4. CONCLUSION

Semiconducting pyrite was successfully deposited on glass substrate from a single source precursor($FeS_2CN(Et)_2)_3$) using AACVD. The p-XRD patterns of the deposited films show that polycrystalline pure pyrite is formed at 300^oC whereas at 350^oC, 400^oC and 450^oC polycrystalline mixture of pyrite and marcasite is formed. We also observed that the temperature of the glass substrate has significant effect on the iron:sulphur ratio of the deposited films. The iron:sulphur ratio of 48:52, 50:50, 60:40 and 70:30 were obtained at 300^oC, 350^oC, 400^oC and 450^oC respectively. This shows that at high deposition temperature, semiconducting pyrite film becomes metallic pyrite film. These results show that iron sulphide minerals are typified by a range of significant temperature induced composition and phase transformation.

ACKNOWLEDGEMENT

The authors are grateful to Tertiary Education Trust Fund (TETFund) for sponsoring this research work. Many thanks to Dr. Chris Wilkinson, Michael Faulkner and Gary Harrison of the University of Manchester for their time in training us on how to use various machines in the school of material sciences

REFERENCE

1. Hopfner C, Ellmer K, Ennaoui A, Pettenkofer C, Fiechter S, Tributsch H. (1995). Journal of Crystal Growth.151.
2. Puthussery James, Sean Seefeld, Nicholas Berry, Markelle Gibbs and Matt Law. (2011). Journal of the American Chemistry Society. 133, 716.
3. Ramasamy K., Malik M.A., Helliwell M., Tuna F., and O'Brien P. (2010). Inorganic Chemistry 49, 8495
4. Nicholas Berry, Ming Cheng, Craig L. Perkins, Moritz Limpinsel, Jonh C. Hemminger and Matt Law (2012), Adv. Energy Mater, 2, 1124-1135
5. Ennaoui, A.; Tributsch, H. Sol. Energy Mater. 1986, 14, 461.,
6. Smestad, G.; Ennaoui, A.; Fiechter, S.; Tributsch, H.; Hofmann, W. K.; Birkholz, M.; Kautek, W. Sol. Energy Mater. Sol. Cells 1990, 20, 149.
7. Ahmed LutfiAbdelhady,† Mohammad A. Malik, Paul O'Brien,* and Floriana Tuna, (2012), J. Phys. Chem. 116, 2253–2259.
8. Wadia, A.; Alivisatos, A. P.; Kammen, D. M. Environ. Sci. Technol. 2009, 43, 2072–2077.
9. Ferrer, I.J., Nevskaia, D.M., Heras, C., and Sanchez, C., 1990, Solid State Commun., 74, 913.
10. Rezig, B., Dahman, H., and Kenzari, M., 1992, Renewable Energy, 2, 125.
11. Birkholz, M., Lichtenberger, D., Hopfner, C., and Fiechter, S., 1992, Sol. Energy Mater. Sol. Cells, 27, 243.
12. Willeke, G., Blenk, O., Kloc, Ch., and Bucher, E., 1992, J. Alloys Compd., 178, 181.
13. Nakamura, S. and Yamamoto, A., 2001, Sol. Energy Mater. Sol. Cells, 65, 79.
14. Bronold, M., Kubala, S., Pettenkofer, C., and Jaegermann, W., 1997, Thin Solid Films, 304, 178.
15. Smestad G, Da Silva A, Tributsch H, Fiechter S, Kunst M, Meziani N, Birkholz M. (1989). Solar Energy Materials. 18, 299.
16. Ennaoui A, Schlichtlorel G, Fiechter S, Tributsch H. (1992). Solar Energy Materials and Solar Cells. 25, 169.
17. Steinhagen Chet, Taylor B. Harvey, C. Jackson Stolle, Justin Harris, and Brian A. Korgel. (2012). Journal of Physical Chemistry Letters. 3, 2352.

18. Ouertani B, Ouerfelli J, Saadoun M, Bessais B, Ezzaouia H, Bernede J.C. (2005). Material Characterization. 54, 431.
19. Bausch S, Sailer B, Keppner H, Willeke G, Bucher E, Frommeyer G. (1990). Applied Physics Letters. 25, 57.
20. Akhtar M., Akhtar J., Malik M.A, O'Brien P., Tuna F., Raftery J., Helliwell M.,(2011) Journal of Materials Chemistry 21, 9737.
21. Malik M.A, Revaprasadu N., O'Brien P., (2001) Chemistry of Materials 13, 913.
22. Nair P.S., Radhakrishan T.R.N., Kolawole G.A. (2001) Journal of Material Chemistry 11, 1555.
23. MasoodAkhtar, Ahmed LuftiAbdelhady, M. Azad Malik, and Paul O'Brien. (2012). Journal of Crystal Growth. 346, 106.
24. Chunggaze M., Malik M.A and O'Brien P. (1997), Advanced Materials for Optics and Electronics. 7, 311.